Dovepress

ORIGINAL RESEARCH

Ciprofol Ameliorates Myocardial Ischemia/Reperfusion Injury by Inhibiting Ferroptosis Through Upregulating HIF-1α

Jun Ding[1–3,]*, Bi-Ying Wang[1,2,]*, Yu-Fan Yang[1,2,]*, Ling-Yu Kuai[1,2], Jing-jie Wan[1,2], Mian Zhang [1,2], Hai-Yan Xia[3], Yao Wang[3], Zhong Zheng[3], Xiao-Wen Meng [1,2], Ke Peng [1,2], Fu-Hai Ji [1,2]

[1]Department of Anesthesiology, First Affiliated Hospital of Soochow University, Suzhou, Jiangsu, People's Republic of China; [2]Institute of Anesthesiology, Soochow University, Suzhou, Jiangsu, People's Republic of China; [3]Department of Anesthesiology, Taicang First People's Hospital, Taicang, Jiangsu, People's Republic of China

*These authors contributed equally to this work

Correspondence: Ke Peng; Fu-hai Ji, Email pengke0422@163.com; jifuhaisuda@163.com

Purpose: Ciprofol is a novel intravenous anesthetic that has been increasingly used in clinical anesthesia and sedation. Studies suggested that ciprofol reduced oxidative stress and inflammatory responses to alleviate cerebral ischemia/reperfusion (I/R) injury, but whether ciprofol protects the heart against I/R injury and the mechanisms are unknown. Herein, we assessed the effects of ciprofol on ferroptosis during myocardial I/R injury.

Methods: Experimental models of myocardial I/R injury in mice (ischemia for 30 min and reperfusion for 24 h) and hypoxia/ reoxygenation (H/R) injury in H9c2 cardiomyocytes (hypoxia for 6 h followed by 6 h of reoxygenation) were established. Ciprofol was used prior to ischemia or hypoxia. Echocardiography, myocardial TTC staining, HE staining, DAB-enhanced Perl's staining, transmission electron microscopy, FerroOrange staining, Liperfluo staining, JC-1 staining, Rhodamine-123 staining, DCFH-DA staining, and Western blot were performed. Cell viability, serum cardiac enzymes, and oxidative- and ferroptosis-related biomarkers were measured. HIF-1α siRNA transfection and the specific inhibitor BAY87-2243 were utilized for mechanistic investigation.

Results: Ciprofol treatment reduced myocardial infarct area and myocardium damage, alleviated oxidative stress and mitochondrial injury, suppressed Fe^{2+} accumulation and ferroptosis, and improved cardiac function in mice with myocardial I/R injury. Ciprofol also increased cell viability, attenuated mitochondrial damage, and reduced intracellular Fe^{2+} and lipid peroxidation in cardiomyocytes with H/R injury. Ciprofol enhanced the protein expression of HIF-1α and GPX4 and reduced the expression of ACSL4. Specifically, the protective effects of ciprofol against I/R or H/R injury were abolished by downregulating the expression of HIF-1α using siRNA transfection or the inhibitor BAY87-2243.

Conclusion: Ciprofol ameliorated myocardial I/R injury in mice and H/R injury in cardiomyocytes by inhibiting ferroptosis via the upregulation of HIF-1α expression.

Keywords: ciprofol, myocardial ischemia/reperfusion injury, ferroptosis, oxidative stress, HIF-1α, GPX4/ACSL4

Introduction

Myocardial infarction is a leading cause of cardiac arrest in middle-aged and elderly people worldwide.[1,2] Timely and effective reperfusion to myocardium is the standard treatment. However, restoration of blood flow paradoxically leads to ischemia/reperfusion (I/R) injury.[3,4] Preventing death of cardiomyocytes is crucial for preserving cardiac function after myocardial reperfusion.[5–7] While many studies have explored the possible underlying mechanisms, preventing or reducing myocardial I/R injury in clinical settings is still challenging.

Ciprofol (HSK3486) is a novel intravenous anesthetic agent developed from propofol with an enhanced chemical structure.[8] Ciprofol is currently being used for sedation and anesthesia in endoscopic procedures,[9,10] for anesthesia induction and maintenance,[11] and for sedation in critically ill patients with mechanical ventilation.[12,13] Ciprofol has

a good sedative efficacy comparable to propofol and provides stable hemodynamics and respiratory status.[14] Previous studies have suggested that propofol alleviated I/R- and drug-induced myocardial injury.[15,16] However, whether ciprofol would offer cardioprotection against I/R injury and the specific mechanisms are not understood.

Ferroptosis is a type of cell death characterized by the accumulation of iron-dependent lipid peroxides.[17] Recent studies have shown the critical role of ferroptosis in myocardial I/R injury.[18,19] Hypoxia-inducible factor-1α (HIF-1α) is a key transcription factor related to ferroptosis.[20–22] Under hypoxic conditions, HIF-1α expression is increased, activating the protective signaling pathways to mitigate cell damage.[23] Glutathione peroxidase 4 (GPX4) and Acyl-CoA synthetase long chain family member 4 (ACSL4) are key regulators in the process of ferroptosis.[20,24] In this study, we investigated whether ciprofol could inhibit ferroptosis to protect the heart by regulating HIF-1α in mice with myocardial I/R injury and in cultured cardiomyocytes with hypoxia/reoxygenation (H/R) injury.

Materials and Methods
Cell Culture and H/R Injury

H9c2 cardiomyocytes were purchased from Cellverse Bioscience Technology Co., Ltd. and cultured in standard Dulbecco's modified eagle medium (DMEM) supplemented with 10% fetal bovine serum (FBS) and 1% penicillin/ streptomycin under a controlled condition (humidified, 37°C, and 5% CO_2) for 24 h. Subsequently, the medium was replaced by a glucose-free medium (Procell, Wuhan, China), and the cells were exposed to a hypoxic environment (95% N_2 and 5% CO_2) at 37°C for 6 h. After hypoxia, the cells were cultured in the normal condition for 6 h of reoxygenation.

In part I, the cultured cells were treated with ciprofol at concentration gradients (1, 5, 10, 50, and 100 μM) in the normal condition (n = 5). Next, ciprofol (1, 5, 10, 50, and 100 μM) was added into the medium before hypoxia (n = 5). Ciprofol at a final concentration of 10 μM was used in the following parts. In part II, the cells were divided into 3 groups (control, H/R, and H/R + ciprofol; n = 4–6). In part III, short interfering RNA (siRNA) targeting HIF-1α (si-HIF-1α) or negative control (si-NC) was used. The cells were divided into 4 groups (H/R, H/R + ciprofol, H/R + ciprofol + si-HIF -1α, and H/R + ciprofol + si-NC; n = 4–6). The schematic diagram is shown in Figure 1A.

Mouse Myocardial I/R Injury

The mouse study was approved by the Animal Ethics Committee of Soochow University Animal Care (WDRM-20200713). All animal care and experimental procedures were conducted in compliance with the Guidelines for the Care and Use of Laboratory Animals. Healthy SPF-C57BL/6 male mice (18–23 g and 8–10 weeks) were procured from the Cavens Biogle Model Animal Research Co., Ltd. Mice were housed in a standard condition (temperature 22–25°C, humidity 40–60%, and a 12-h light/dark cycle) and provided with food and water, with a 12-h fasting period before the experiments.

The mouse model of myocardial I/R injury was induced as follows. After intraperitoneal injection of 1% sodium pentobarbital (50 mg/kg), mice were endotracheally intubated and connected to a rodent ventilator. The heart was exposed through a small chest incision. Left anterior descending coronary artery was sutured with 6–0 silk thread under microscopy. The blanched anterior wall of the left ventricle and changes in electrocardiography confirmed successful myocardial ischemia. After 30 min of ischemia, the suture was loosened. The restoration of ST segment and color in the anterior wall indicated successful reperfusion. Following 24 h of reperfusion, blood and heart samples were harvested.

Figure 1B depicts the schematic diagram of mouse experiments. Using a computer-generated randomization list, the mice were randomized into 3 groups in part I (sham, myocardial I/R, and I/R + ciprofol; n = 4–8) and 4 groups in part II (sham, myocardial I/R, I/R + ciprofol, and I/R + ciprofol + BAY87-2243; n = 4–6). The mice in the sham group underwent the same procedures without ligation. The mice in the I/R + ciprofol group received intraperitoneal injection of ciprofol (10 mg/kg; HSK3486, Haisco Pharmaceutical Group Co., Ltd) 1 h prior to ischemia. The mice in the I/R + ciprofol + BAY87-2243 group received intragastric administration of BAY87-2243 (9 mg/kg; APExBIO) daily for 3 days before ischemia. BAY87-2243 is an inhibitor of HIF-1α used in recent studies.[25,26]
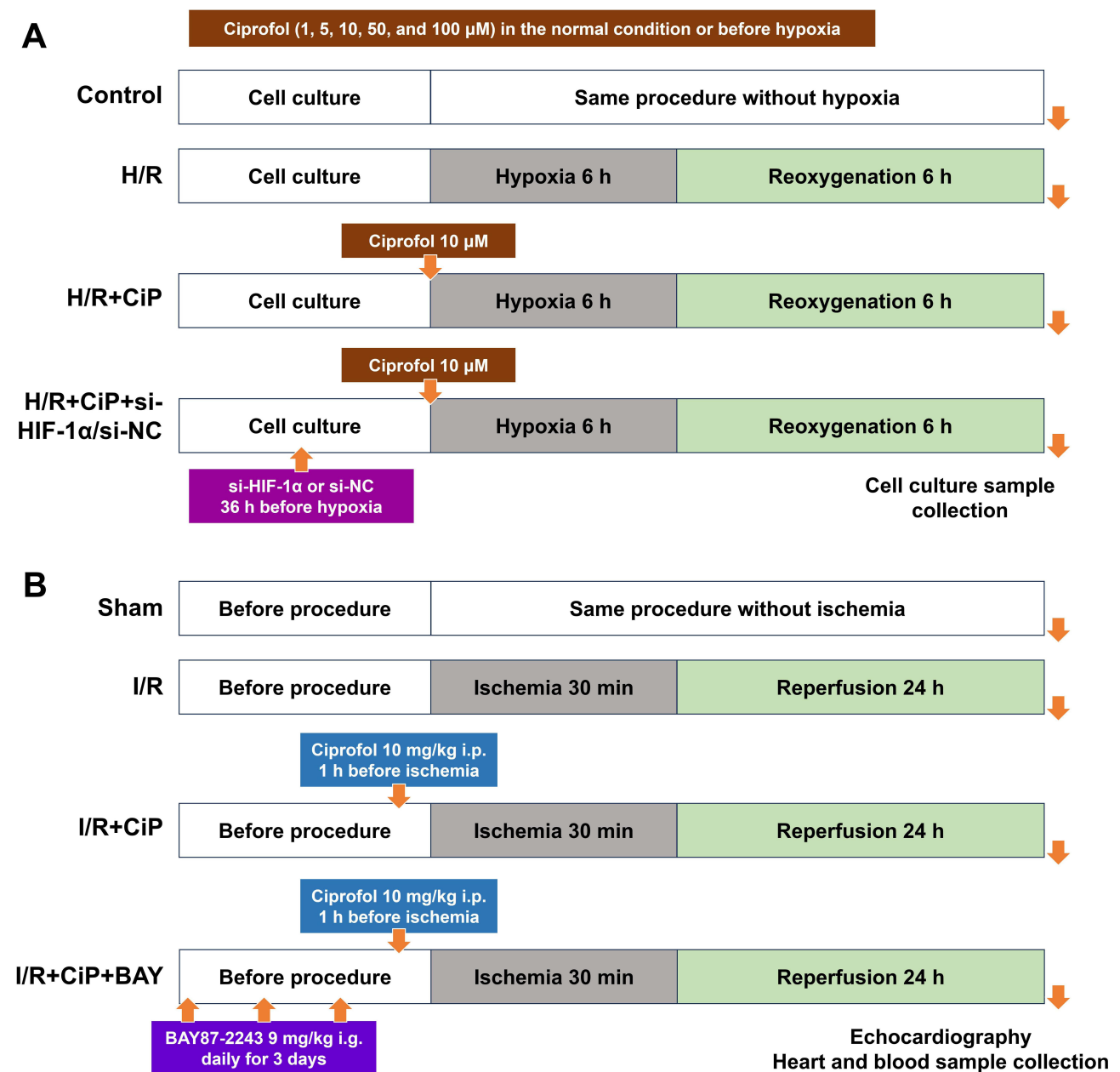
A

Ciprofol (1, 5, 10, 50, and 100 μM) in the normal condition or before hypoxia

Control	Cell culture	Same procedure without hypoxia

H/R	Cell culture	Hypoxia 6 h	Reoxygenation 6 h

Ciprofol 10 μM

H/R+CiP	Cell culture	Hypoxia 6 h	Reoxygenation 6 h

Ciprofol 10 μM

H/R+CiP+si-HIF-1α/si-NC	Cell culture	Hypoxia 6 h	Reoxygenation 6 h

si-HIF-1α or si-NC
36 h before hypoxia

Cell culture sample collection

B

Sham	Before procedure	Same procedure without ischemia

I/R	Before procedure	Ischemia 30 min	Reperfusion 24 h

Ciprofol 10 mg/kg i.p.
1 h before ischemia

I/R+CiP	Before procedure	Ischemia 30 min	Reperfusion 24 h

Ciprofol 10 mg/kg i.p.
1 h before ischemia

I/R+CiP+BAY	Before procedure	Ischemia 30 min	Reperfusion 24 h

BAY87-2243 9 mg/kg i.g.
daily for 3 days

Echocardiography
Heart and blood sample collection

Figure 1 Schematic diagram. (**A**) H9c2 cardiomyocytes underwent H/R injury. First, cells were treated with ciprofol (1, 5, 10, 50, and 100 μM) in the normal condition or before hypoxia. Next, ciprofol (10 μM) was used, and si-HIF-1α or si-NC was transfected 36 h before ciprofol treatment. At the end of reoxygenation, cell culture samples were collected. (**B**) Mice underwent myocardial I/R injury. Ciprofol (10 mg/kg i.p.) was given 1 h before ischemia. BAY87-2243 (9 mg/kg i.g.) was administered daily for 3 days prior to ischemia. At the end of reperfusion, echocardiography was conducted, and heart and blood samples were collected.

Cell Transfection

The siRNAs were synthesized by Guangzhou Ribo Biotechnology Co., Ltd. H9c2 cells were seeded in a well plate and cultured overnight. Following the instructions, the vector was transfected using a 1:3 volume ratio of DNA to Lipomaster 2000 transfection reagent (Novizan, Nanjing, China). After 6 h of transfection, the culture medium was replaced. The cells were then cultured for an additional 30 h, and the experimental interventions were carried out.

Echocardiography

Mouse cardiac function was assessed at 24 h after myocardial reperfusion using the transthoracic echocardiography (Vevo 2100 ultrasound system). The mice underwent a brief anesthesia with 2% sevoflurane inhalation. After an

appropriate coupling agent was applied, the position of ultrasound probe was adjusted to capture high-quality left ventricular views in both the long and short axes. The left ventricular end-diastolic diameter and left ventricular end-systolic diameter were measured to calculate the left ventricular ejection fraction (LVEF) and left ventricular fractional shortening (LVFS). Each mouse underwent three measurements, and the average value was recorded.

Myocardial Infarct Area

The 2,3,5-Triphenyltetrazolium chloride (TTC) staining is a well-established approach to assess the myocardial infarct area. Following reperfusion, mice were subjected to re-tightening of the ligation line at the initial site of heart ligation. Subsequently, Evans blue dye was administered via the tail vein. Once the entire mouse body exhibited a blue coloration, the heart was excised, rapidly frozen for 30 min, and evenly sectioned below the ligation line. The sections were stained with TTC dye for 20 min and then imaged for the calculation of the infarct area.

Hematoxylin-and-Eosin (HE) Staining

Mouse heart specimens were collected and fixed in 4% paraformaldehyde for 24 h. The myocardial tissue was dehydrated, embedded in paraffin, sectioned into 6-μm thickness, and stained with HE (Servicebio, Wuhan, China). Subsequently, tissue morphology images were captured using an Olympus microscope.

Diaminobenzidine (DAB)-Enhanced Perl's Staining

Briefly, paraffin sections of the myocardium were dewaxed, washed, incubated in freshly prepared Perl's solution for 30 min. Next, the sections were rinsed with distilled water and stained with DAB chromogenic solution for 5 min, followed by hematoxylin staining of the nucleus for 1 min. Subsequently, images were collected under a microscope for analysis. Iron deposition sites in tissues appear brown after DAB-enhanced Perl's staining.

Transmission Electron Microscopy

The mouse hearts were collected and the myocardial tissues below the ligation line were cut into about 1-mm^3 size. Subsequently, the tissues were fixed in electron microscope fixative (G1102, Servicebio, Wuhan, China) at room temperature for 2 h, followed by fixation at 4°C for 24 h. Afterwards, the myocardial tissues were cut into ultra-thin sections for imaging and analysis using an electron microscope.

Serum Cardiac Enzymes

The serum samples were collected by centrifuging blood at the end of reperfusion. Serum levels of cardiac enzymes including creatine kinase isoenzyme MB (CK-MB) and cardiac troponin I (cTnI) were measured using the enzyme-linked immunosorbent assay (ELISA) kits (Elabscience, USA). The OD values were recorded by a microplate reader, and the concentrations of CK-MB and cTnI were calculated by using a standard curve.

Cell Viability

Cell viability was assessed using the Cell Counting Kit-8 (CCK-8) (APExBIO, TX, USA) according to the manufacturer's instructions. Briefly, the H9c2 cells were seeded evenly in a 96-well plate. Following the experimental treatments, 10 μL of CCK-8 reagent was added to each well. The cells were incubated in darkness for 2 h, and the absorbance value at 450 nm was recorded using a microplate reader.

FerroOrange Staining

Intracellular Fe^{2+} levels were assessed using the FerroOrange probe (Maokang, Shanghai, China). The orange iron working solution was added to achieve a final concentration of 1 μM, followed by incubation at 37°C for 30 min. Then, the cells were examined under microscopy.

Liperfluo Staining

Intracellular ferroptosis-related lipid peroxidation was assessed using the Liperfluo probe (DOJINDO, L248, Japan). Following H/R and experimental treatment, the cells were cultured in serum-free medium. The Liperfluo working solution was added to reach a final concentration of 5 μM, followed by incubation at 37°C for 30 min. Subsequently, the cells were washed and observed under microscopy.

Intracellular Reactive Oxygen Species (ROS)

Intracellular ROS level was measured using the DCFH-DA probe (Beyotime, Shanghai, China). At the end of cell experiment, the DCFH-DA solution was added to the DMEM culture without FBS at a final concentration of 1 μM, followed by incubation in the dark for 30 min. The cells were then washed with PBS and the nuclei were stained with Hoechst 33342. Finally, the cells were observed under a fluorescence microscope.
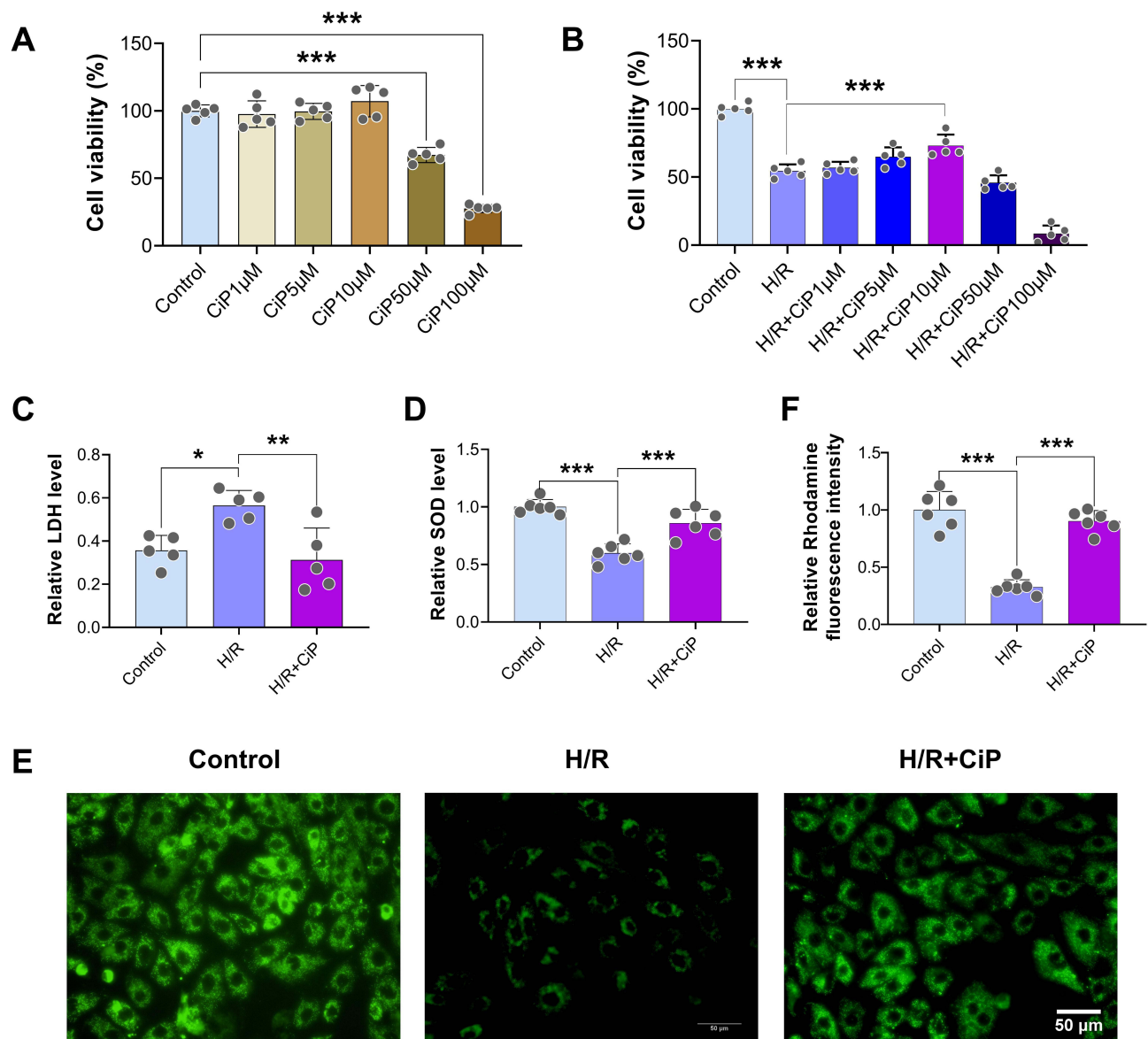
Figure 2 Ciprofol attenuated H/R-induced injury in H9c2 cardiomyocytes. (**A**) Cell viability after ciprofol (1, 5, 10, 50, and 100 μM) in the normal condition. (**B**) Cell viability after ciprofol (1, 5, 10, 50, and 100 μM) during H/R. (**C** and **D**) Levels of LDH and SOD. Ciprofol (10 μM) was added 1 h before H/R. (**E** and **F**) Representative images and fluorescence intensity of Rhodamine 123 staining. Ciprofol (10 μM) was added 1 h before H/R. Scale bar = 50 μm. Data are shown as mean ± SD (n = 5–6). *$P < 0.05$, **$P < 0.01$, ***$P < 0.001$.

Mitochondrial Membrane Potential

Rhodamine-123 (Beyotime, Shanghai, China) and JC-1 staining (Beyotime, Shanghai, China) were utilized to assess mitochondrial membrane potential. Following cell treatment, Rhodamine-123 or JC-1 working solution was added to the DMEM culture without FBS (a final concentration of 1 μM), followed by incubation at 37°C in the dark for 30 min. Subsequently, excess dye was removed, and images were captured using an inverted fluorescence microscope. In Rhodamine-123 staining, the weakening of green fluorescence signal on mitochondria indicates decreased mitochondrial membrane potential in damaged cells. In JC-1 staining, an increase in green fluorescence signal and a decrease in red fluorescence signal suggest the dissipation of mitochondrial membrane potential and mitochondrial damage.

Measurement of Oxidative- and Ferroptosis-Related Biomarkers

The oxidative- and ferroptosis-related biomarkers included lactate dehydrogenase (LDH), superoxide dismutase (SOD), lipid peroxidation (LPO), malondialdehyde (MDA), glutathione (GSH), and ferrous ions (Fe^{2+}). LDH is a crucial enzyme in the redox reaction chain, and SOD is an important antioxidant metalloenzyme. Following cellular damage, the level of LDH increases, whereas the level of SOD decreases. MDA and LPO are metabolites derived from unsaturated fatty acids, and GSH functions as an antioxidant. During cellular damage, both MDA and LPO accumulate, accompanied by a reduction in
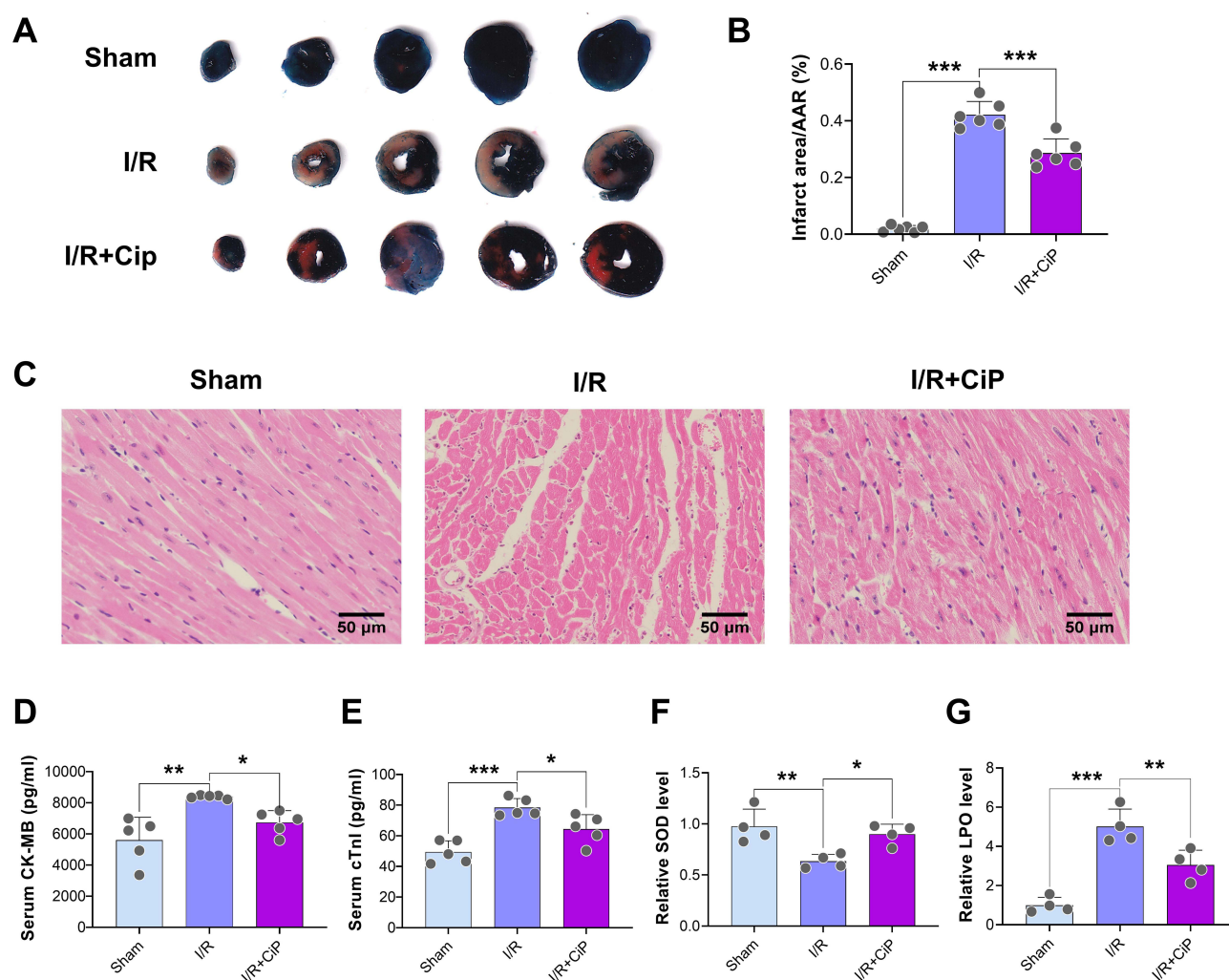
Figure 3 Ciprofol alleviated I/R-induced myocardial injury in mice. Ciprofol (10 mg/kg i.p.) was given 1 h prior to ischemia. (**A** and **B**) Representative myocardial TTC staining images and quantification of infarction size. (**C**) Representative HE staining images of myocardium. Scale bar = 50 μm. (**D** and **E**) Serum levels of cardiac enzymes (CK-MB and cTnI). (**F** and **G**) Serum levels of SOD and LPO. Data are shown as mean ± SD (n = 4–6). *$P < 0.05$, **$P < 0.01$, ***$P < 0.001$.

GSH. Following the manufacturers' instructions, the levels of these biomarkers in mouse heart samples and cell culture supernatants were assessed using the specific assay kits (Nanjing Jiancheng Bioengineering Institute, China).

Western Blot

Myocardial tissues and H9c2 cells were lysed using the RIPA lysis buffer (Beyotime, Shanghai, China). The protein concentration was determined using the bicinchoninic acid kit (Beyotime, Shanghai, China). The proteins were separated via sodium dodecyl sulfate-polyacrylamide gel electrophoresis (SDS-PAGE) on a 10% gel and transferred to a polyvinylidene fluoride (PVDF) membrane. Following a 2-h block with 5% skim milk at room temperature, the membranes were incubated at 4°C overnight with the specific primary antibodies: HIF-1α (340462, Zenbio, China), ACSL4 (CY10198, Abways, China), GPX4 (CY6959, Abways, China), and GAPDH (FD0063, Fdbio Science, China). On the next day, the membranes were incubated with a secondary antibody (1:4000, CoWin, China) for 2 h at room temperature and visualized using an enhanced chemiluminescence detection kit (New Cell Molecular Biotechnology, Suzhou, China). The expression of proteins was quantified using the Image J software.

Immunofluorescence Staining

Mouse heart specimens were collected and fixed in a 4% paraformaldehyde solution for 24 h, embedded in paraffin, and sectioned into 6-μm thick slices. After dewaxing, citric acid was used to retrieve tissue antigens, followed by membrane permeabilization with low-concentration Triton. Subsequently, donkey serum was applied to block non-specific binding. The slices were then incubated with the primary HIF-1α antibody (340462, Zenbio, China), followed by incubation and staining with a fluorescence-conjugated secondary antibody. DAPI was used to stain the nuclei. An antifade reagent was added and the slides were sealed. Slices were observed using a fluorescence microscope. Immunofluorescence intensity was analyzed using the ImageJ software.

Statistical Analysis

All experimental data are presented as mean ± standard deviation (SD). Study groups (n ≥ 5) were compared using one-way analysis of variance with Dunnett correction for multiple comparisons. Small study groups (n < 5) were compared using the permutation test which does not rely on distributional assumptions. Statistical analysis was conducted using the GraphPad Prism 9 software (GraphPad, San Diego, CA, USA) and the R software (version 3.6.0, R Foundation for Statistical Computing, Vienna, Austria). A P value < 0.05 indicates a statistically significant difference.

Results

Ciprofol Reduced Oxidative Injury Induced by H/R in H9c2 Cardiomyocytes

First, we assessed the viability of H9c2 cardiomyocytes after ciprofol treatment at concentration gradients (1, 5, 10, 50, and 100 μM) in the normal condition and during H/R (Figure 2A and B). We found that ciprofol 10 μM exerted the optimal protective effects, while ciprofol at higher concentrations (50 and 100 μM) reduced cell viability in the normal condition and failed to rescue the viability following H/R. Thus, we utilized ciprofol 10 μM in the subsequent cell experiments.

Next, we found that H/R significantly increased the level of LDH and decreased the level of SOD in the supernatant of cell cultures, indicating substantial oxidative damage caused by H/R, whereas ciprofol attenuated this damage (Figure 2C and D). Additionally, the Rhodamine 123 (a probe of mitochondrial membrane potential) staining results showed that ciprofol significantly attenuated the H/R-induced mitochondrial damage (Figure 2E and F).

Ciprofol Alleviated Oxidative Stress and Myocardial I/R Injury in Mice

First, we performed the TTC staining to show that ciprofol treatment reduced the infarct area after myocardial I/R injury (Figure 3A and B). The HE staining sections indicated that ciprofol mitigated I/R-induced myocardium tissue damage (Figure 3C). The analyses of serum CK-MB and cTnI suggested that ciprofol treatment significantly reduced myocardial I/R injury (Figure 3D and E).

Next, the serum SOD level was decreased and LPO was increased during myocardial I/R injury, which was rescued by ciprofol, suggesting that ciprofol protected the mouse hearts against I/R-induced oxidative stress damage (Figure 3F and G).

Furthermore, we conducted echocardiography in mice. The results showed that ciprofol significantly improved cardiac function, as reflected by higher values of LVEF and LVFS in the ciprofol treatment group than in the myocardial I/R group (Figure 4A–C).

Ciprofol Suppressed Ferroptosis and Enhanced HIF-1α Expression During H/R Injury in Cardiomyocytes

First, we used the FerroOrange staining to show a significant decrease in intracellular Fe^{2+} accumulation in cells treated with ciprofol compared with the H/R group (Figure 5A and B). The Liperfluo staining results revealed that ciprofol significantly reduced the intracellular lipid peroxide level during H/R-induced injury (Figure 5C and D). In addition, ciprofol treatment reduced the levels of Fe^{2+} and MDA in the cells (Figure 5E and F).

Next, the Western blot results demonstrated that H/R increased the protein expression of HIF-1α and ACSL4 and reduced the GPX4 expression (Figure 5G–J). With the ciprofol treatment, the expression of HIF-1α was further elevated, and the changes in ACSL4 and GPX4 caused by H/R were partly inhibited by ciprofol.

Ciprofol Inhibited Myocardial I/R-Induced Fe^{2+} Accumulation and Mitochondrial Damage in Mice

First, we investigated whether ciprofol could reduce the accumulation of Fe^{2+} in mouse myocardium during I/R injury. We utilized the Perl's staining to show that myocardial I/R led to a noticeable Fe^{2+} deposition, which was inhibited by ciprofol treatment (Figure 6A).

Next, the transmission electron microscopy was used to analyze the mitochondrial ultrastructure in mouse myocardium. The results showed that mitochondria displayed pyknotic features and a loss of cristae in the myocardial I/R group, whereas ciprofol rescued this mitochondrial damage (Figure 6B).
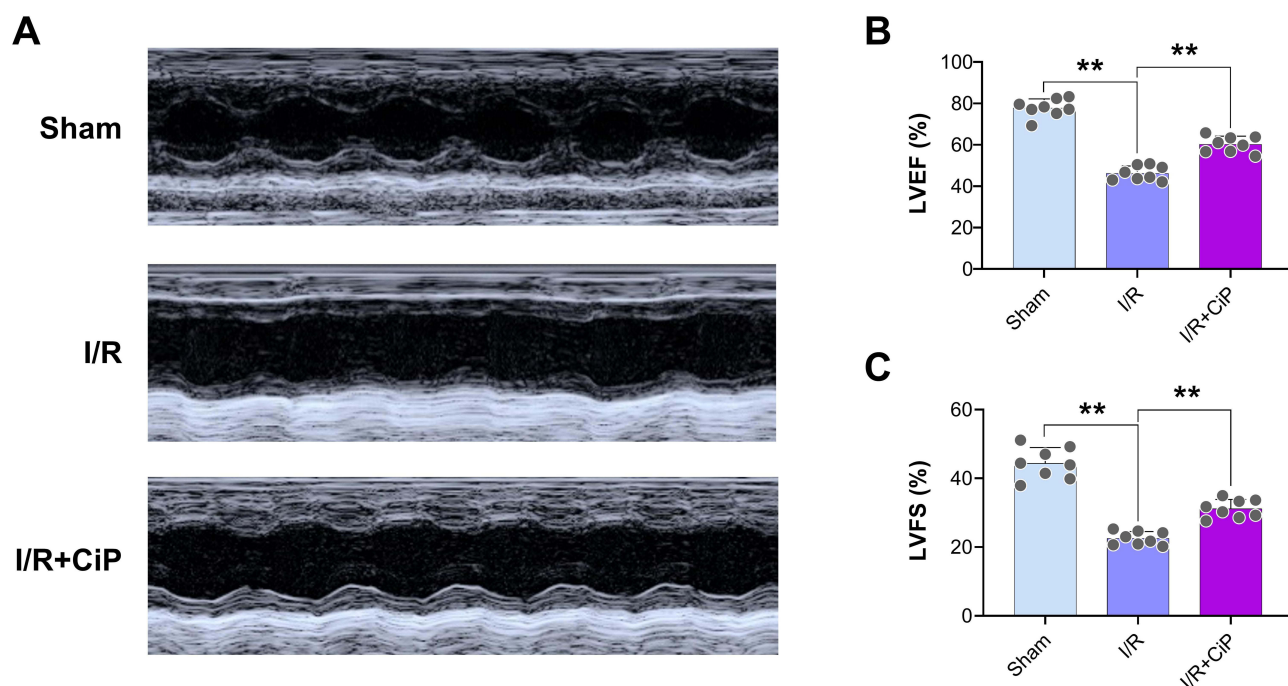

Figure 4 Ciprofol improved cardiac function in mice with myocardial I/R injury. Ciprofol (10 mg/kg i.p.) was given 1 h prior to ischemia. (**A**) Representative echocardiography images. (**B** and **C**) Values of LVEF and LVFS. Data are shown as mean ± SD (n = 8). **$P < 0.01$.
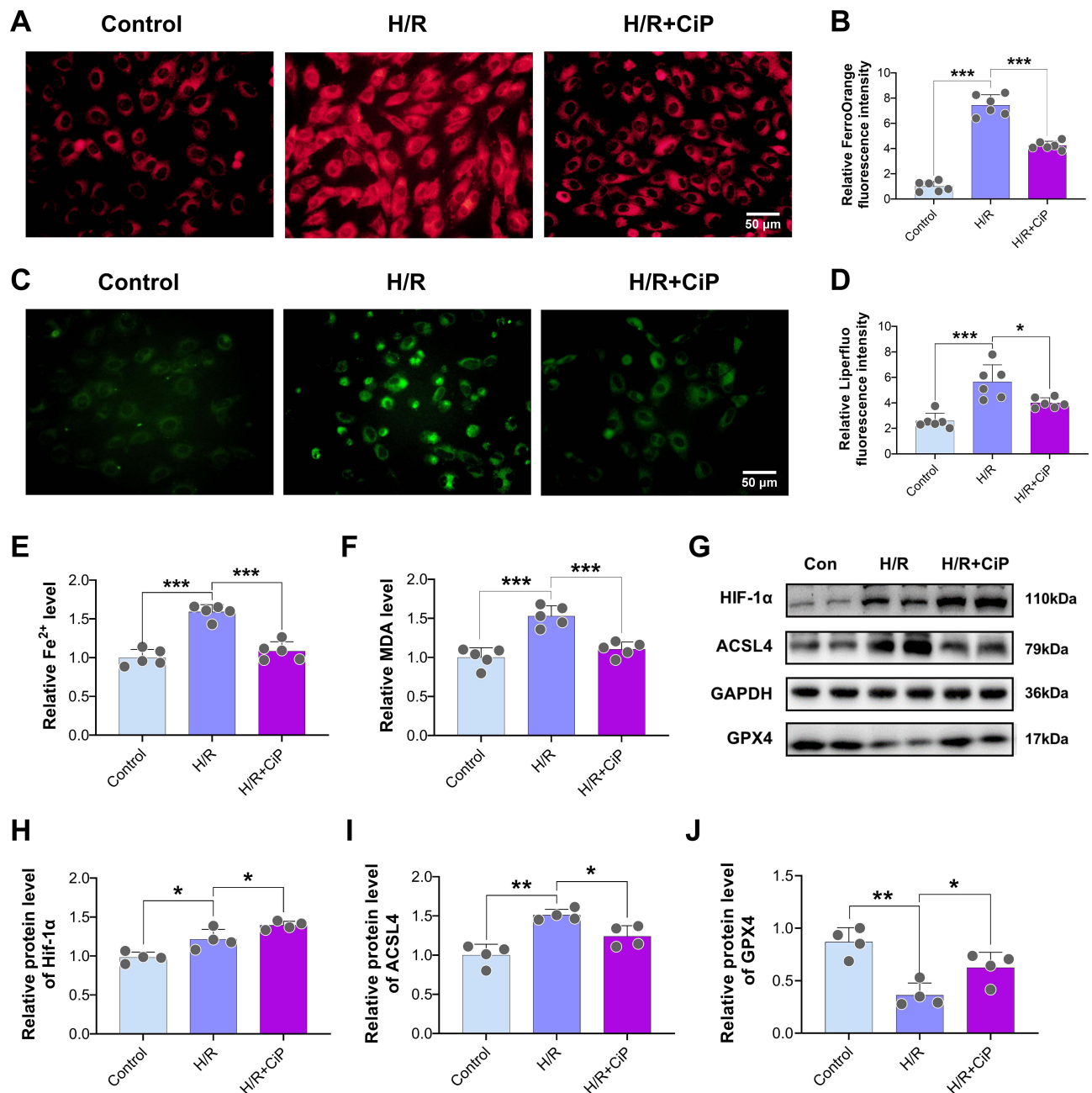
Figure 5 Ciprofol suppressed H/R-induced ferroptosis and increased HIF-1α expression in H9c2 cardiomyocytes. Ciprofol (10 μM) was added 1 h before H/R. (**A** and **B**) Representative images and fluorescence intensity of FerroOrange staining. Scale bar = 50 μm. (**C** and **D**) Representative images and fluorescence intensity of Liperfluo staining. Scale bar = 50 μm. (**E** and **F**) Levels of Fe^{2+} and MDA. (**G–J**) Western blot bands and quantification of HIF-1α, ACSL4, and GPX4 protein expression. Data are shown as mean ± SD (n = 4–6). *$P < 0.05$, **$P < 0.01$, ***$P < 0.001$.

Additionally, we assessed the biomarkers of ferroptosis including Fe^{2+}, MDA, and GSH in the mouse hearts. The findings indicated that ciprofol suppressed the release of Fe^{2+} and MDA and restored the level of GSH during myocardial I/R injury in mice (Figure 6C–E).

Ciprofol Attenuated H/R-Induced Ferroptosis in Cardiomyocytes by Upregulating HIF-1α

First, we explored the role of HIF-1α, a crucial regulatory factor during H/R-induced injury, in the protection of ciprofol against oxidative stress in H9c2 cardiomyocytes. We utilized siRNA to downregulate the expression of HIF-1α. The
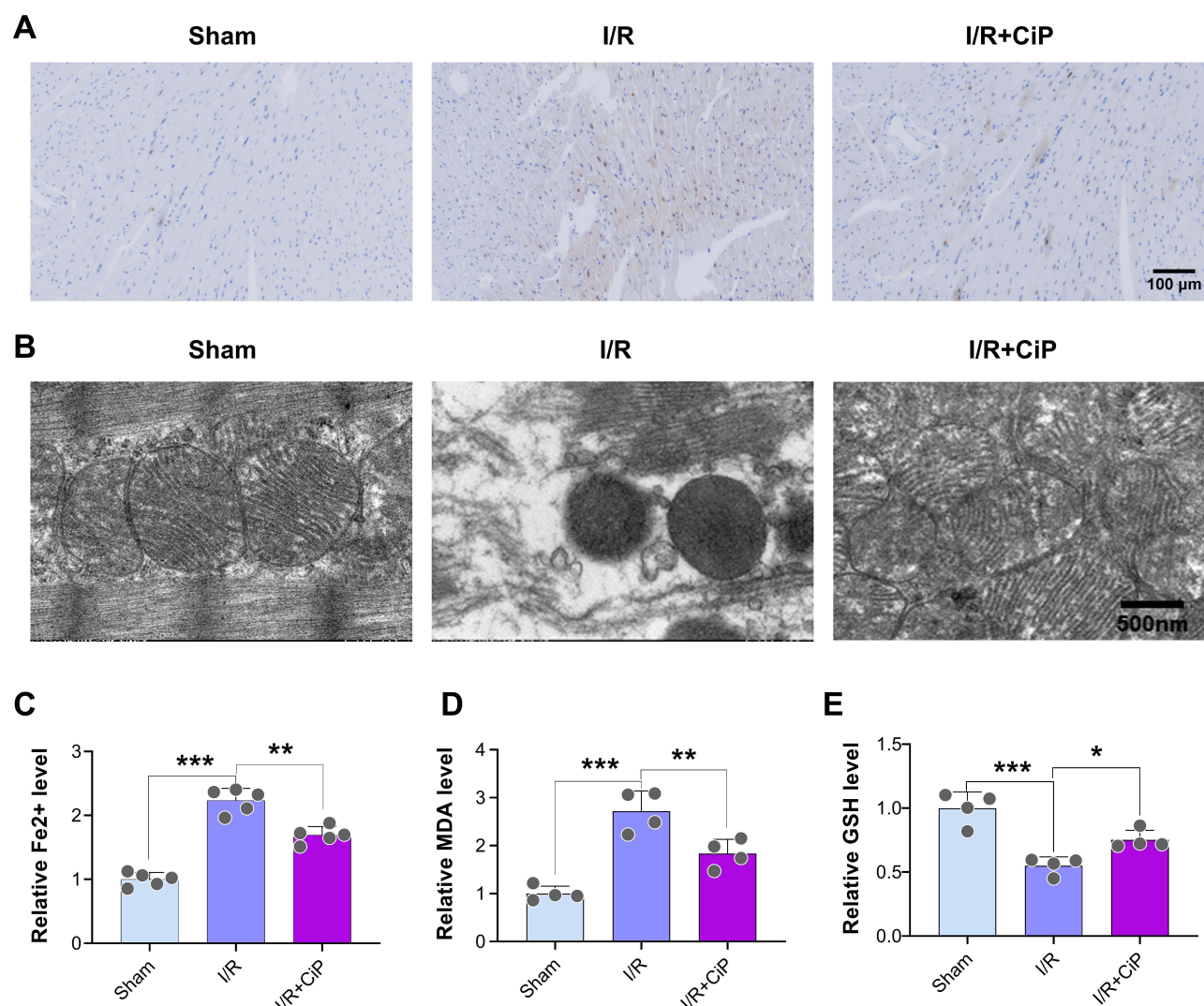
Figure 6 Ciprofol reduced Fe^{2+} accumulation and mitochondrial damage in mice with myocardial I/R injury. Ciprofol (10 mg/kg i.p.) was given 1 h prior to ischemia. (**A**) Representative Perl's staining images of myocardium. Scale bar = 100 μm. (**B**) Representative mitochondrial ultrastructure images under transmission electron microscopy. Scale bar = 500 nm. (**C–E**) Serum levels of Fe^{2+}, MDA, and GSH. Data are shown as mean ± SD (n = 4–5). *$P < 0.05$, **$P < 0.01$, ***$P < 0.001$.

results showed that ciprofol inhibited the release of LDH and LPO and increased the level of SOD in cells subjected to H/R, whereas downregulating HIF-1α reversed these changes (Figure 7A–C).

Next, we performed DCFH-DA staining to show that the intracellular ROS level was reduced by ciprofol during H/R injury, while si-HIF-1α elevated the ROS level (Figure 7D and E). The JC-1 probe was also used to assess the mitochondrial membrane potential of cardiomyocytes. Ciprofol reduced the level of JC-1 monomers (green) and increased JC-1 aggregates (red), suggesting that ciprofol protected the mitochondrial function against H/R injury (Figure 8A–C). However, downregulation of HIF-1α expression abolished the protective effect of ciprofol.

In addition, ciprofol treatment reduced the levels of Fe^{2+} and MDA and increased the level of GSH during H/R cell injury, and these effects were partly blocked by si-HIF-1α (Figure 9A–C). Silencing HIF-1α led to a significant increase in intracellular Fe^{2+} as detected by the FerroOrange staining (Figure 9D and E) and an obvious elevation of intracellular lipid peroxide accumulation assessed using the Liperfluo staining (Figure 9F and G).

Moreover, we performed Western blot to analyze the key protein expression in cells subjected to H/R and after ciprofol treatment and si-HIF-1α. The results showed that ciprofol increased the protein expression of HIF-1α and GPX4 and reduced the expression of ACSL4, while downregulating HIF-1α reversed these effects of ciprofol (Figure 9H–K).
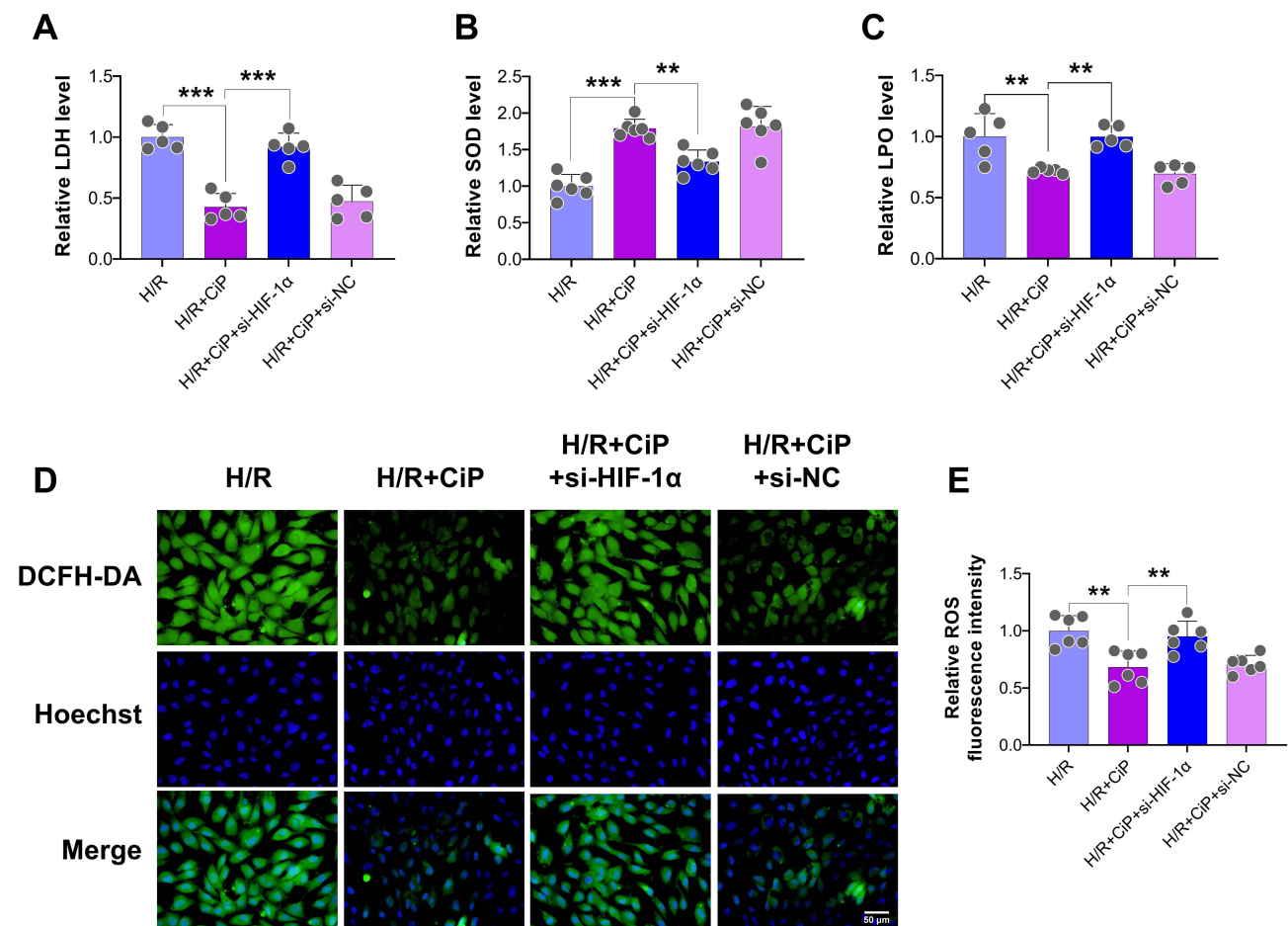
Figure 7 Knockdown of HIF-1α abolished the protective effects of ciprofol against H/R-induced injury in H9c2 cardiomyocytes. si-HIF-1α or si-NC was transfected 36 h before ciprofol (10μM) treatment. (**A–C**) Levels of LDH, SOD, and LPO. (**D** and **E**) Representative DCFH-DA staining images and fluorescence intensity of intracellular ROS. Scale bar = 50 μm. Data are shown as mean ± SD (n = 5–6). **$*P < 0.01$, ***$P < 0.001$.

Ciprofol Mitigated I/R-Induced Myocardial Injury and Ferroptosis in Mice by Upregulating HIF-1α

First, we performed the TTC staining to show that inhibiting HIF-1α by BAY87-2243 reversed the protective effect of ciprofol on I/R-induced myocardial infarction in mice (Figure 10A and B). We then assessed the markers of ferroptosis including Fe^{2+} and GSH in the mouse hearts. The results showed that ciprofol reduced the level of Fe^{2+} and restored the level of GSH during myocardial I/R injury, while these changes were reversed by using the HIF-1α inhibitor BAY87-2243 (Figure 11A and B). The Perl's staining experiment suggested that ciprofol reduced Fe^{2+} deposition during myocardial I/R injury, which was blocked by using BAY87-2243 (Figure 11C).

Next, we used the transmission electron microscopy to observe the ultrastructure of mitochondria in mouse myocardium. Ciprofol treatment mitigated the mitochondrial damage caused by myocardial I/R injury, while inhibition of HIF-1α abolished the protective effect of ciprofol on mitochondria (Figure 11D).

Furthermore, we performed immunostaining experiment in mouse myocardium, showing that the expression of HIF-1α was increased during myocardial I/R injury and was further elevated by ciprofol treatment, whereas the use of BAY87-2243 significantly decreased HIF-1α expression (Figure 12A and B). We also performed Western blot experiment to demonstrate that ciprofol enhanced the protein expression of HIF-1α and GPX4 and reduced the expression of ACSL4 in mice with myocardial I/R injury; however, inhibiting HIF-1α reversed the effects of ciprofol on GPX4 and ACSL4 (Figure 12C–F).
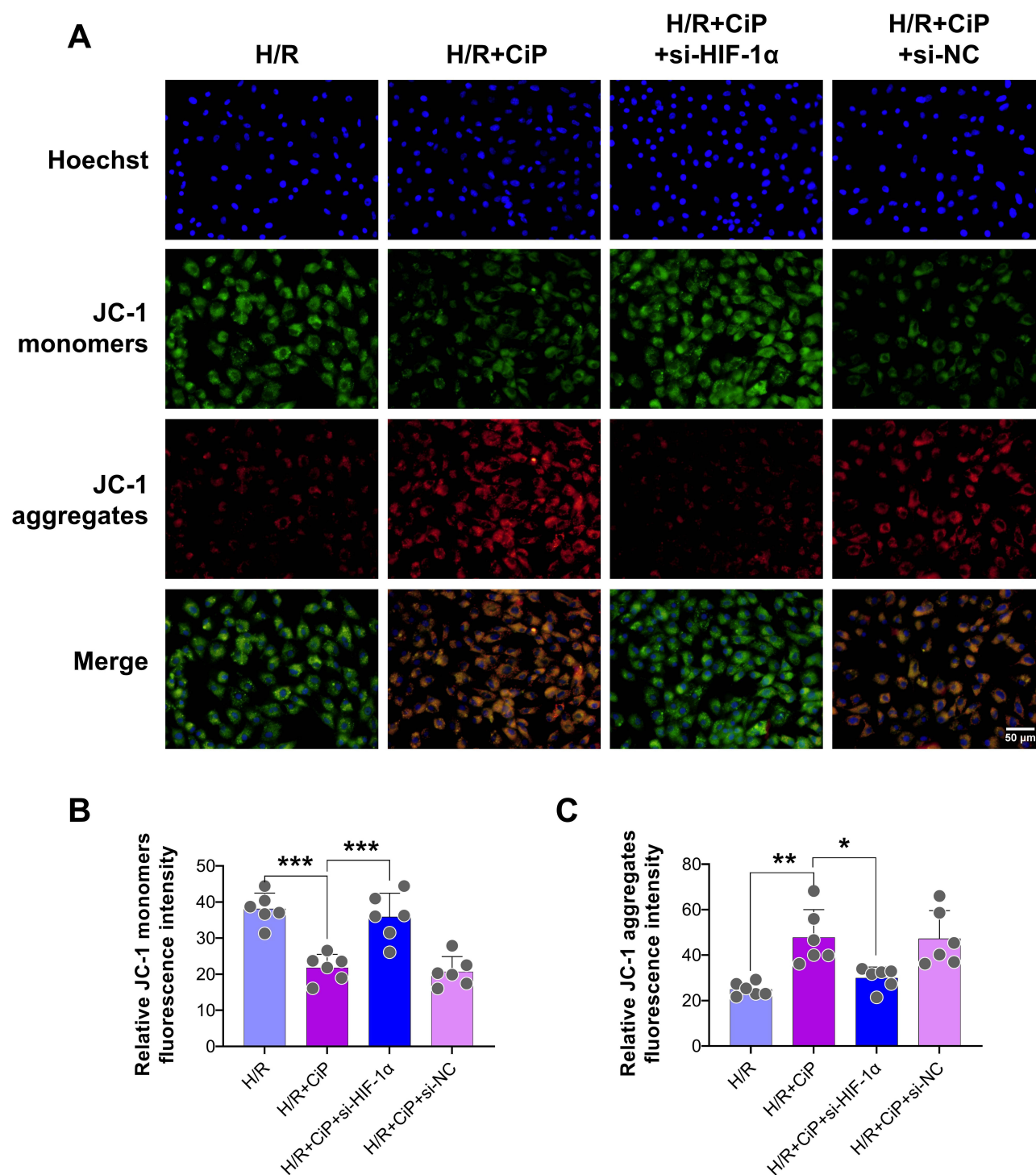
Figure 8 Knockdown of HIF-1α reversed the protective effects of ciprofol on mitochondrial function in H9c2 cardiomyocytes subjected to H/R injury. si-HIF-1α or si-NC was transfected 36 h before ciprofol (10μM) treatment. (**A**) Representative JC-1 staining images showing mitochondrial membrane potential. Scale bar = 50 μm. (**B** and **C**) Fluorescence intensity of JC-1 monomers (green) and aggregates (red). Data are shown as mean ± SD (n = 6). *$P < 0.05$, **$P < 0.01$, ***$P < 0.001$.

Discussion

In this study, we performed both in vivo and in vitro experiments to demonstrate that ciprofol pretreatment significantly reduced I/R-induced injury in mouse hearts and attenuated H/R-induced injury in cultured cardiomyocytes. Moreover, these protective effects of ciprofol were mainly attributable to the inhibition of ferroptosis via activating the expression of HIF-1α and regulating the expression of GPX4/ACSL4.
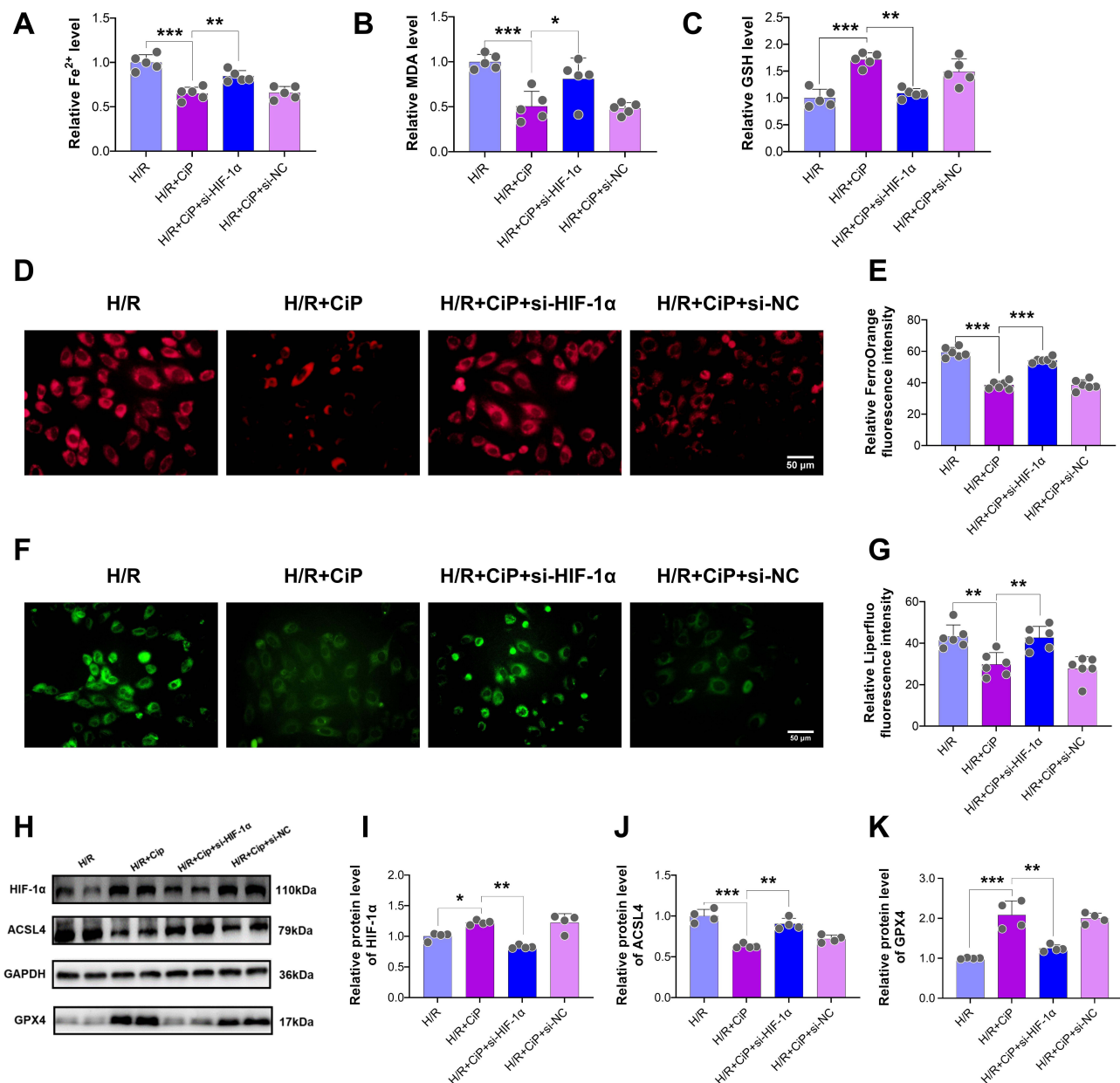
Figure 9 Ciprofol inhibited H/R-induced ferroptosis in H9c2 cardiomyocytes by upregulating HIF-1α. si-HIF-1α or si-NC was transfected 36 h before ciprofol (10μM) treatment. (**A**–**C**) Levels of Fe^{2+}, MDA, and GSH. (**D** and **E**) Representative images and fluorescence intensity of FerroOrange staining. Scale bar = 50 μm. (**F** and **G**) Representative images and fluorescence intensity of Liperfluo staining. Scale bar = 50 μm. (**H**–**K**) Western blot bands and quantification of HIF-1α, ACSL4, and GPX4 protein expression. Data are shown as mean ± SD (n = 4–6). *$P < 0.05$, **$P < 0.01$, ***$P < 0.001$.

Ferroptosis is a distinct form of programmed cell death, which is regulated by iron and characterized by lipid peroxidative damage. Ferroptosis primarily occurs during the reperfusion phase and is a significant contributor to myocardial injury.[18] Studies suggested that inhibiting ferroptosis protected the hearts against I/R injury.[19,27,28] Propofol has been shown to inhibit ferroptosis and reduce myocardial injury by maintaining mitochondrial structure and regulating iron and antioxidant enzyme expression.[29] Our findings revealed that ciprofol reduced iron deposition, suppressed the generation of lipid peroxides, and mitigated mitochondrial damage after I/R- or H/R-induced injury.

Hypoxia-inducible factor is a transcription factor consisting of HIF-α and HIF-β subunits. Mammals have three HIF-α subtypes (HIF-1α, HIF-2α, and HIF-3α). HIF-1α is activated under hypoxic conditions and plays an important role to protect the heart against I/R injury.[30] We showed that ciprofol upregulated the expression of HIF-1α, while down-regulating HIF-1α by si-RNA or its inhibitor BAY87-2243 increased the level of ferroptosis and aggravated myocardial

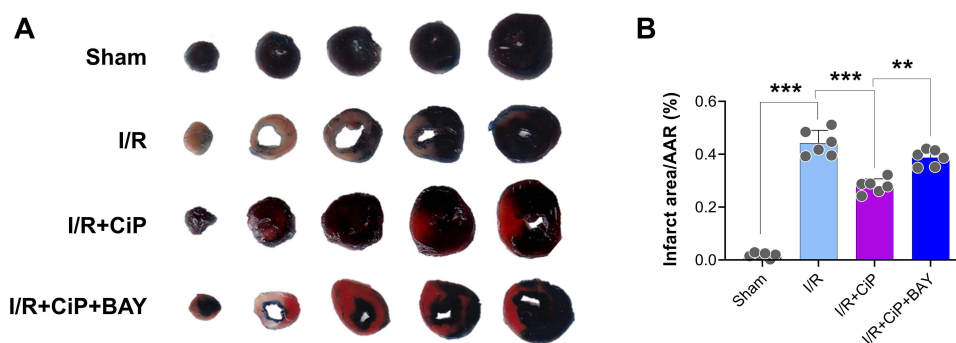**Figure 10** Inhibiting HIF-1α reversed the protective effect of ciprofol on I/R-induced myocardial infarction in mice. BAY87-2243 (9 mg/kg i.g.) was administered daily for 3 days prior to ischemia. (**A**) Representative myocardial TTC staining images. (**B**) Quantification of myocardial infarction size. Data are shown as mean ± SD (n = 6). **$P < 0.01$, ***$P < 0.001$.
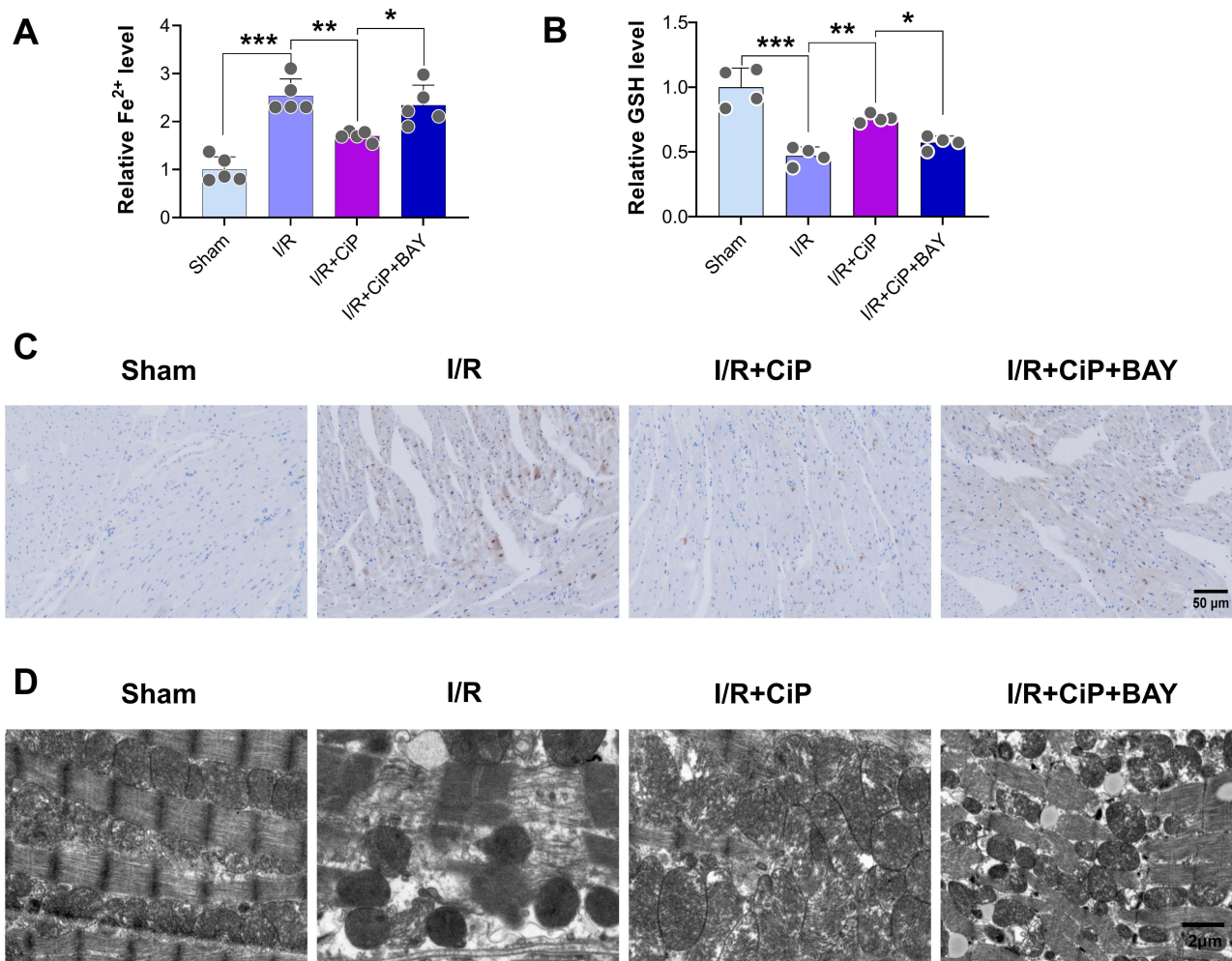

Figure 11 Inhibiting HIF-1α reversed the protective effects of ciprofol on Fe^{2+} accumulation and mitochondrial damage in mice with myocardial I/R injury. BAY87-2243 (9 mg/kg i.g.) was administered daily for 3 days prior to ischemia. (**A** and **B**) Serum levels of Fe^{2+} and GSH. (**C**) Representative Perl's staining in myocardial tissues. Scale bar = 50 μm. (**D**) Representative mitochondrial ultrastructure images under transmission electron microscopy. Scale bar = 2 μm. Data are shown as mean ± SD (n = 4–5). *$P < 0.05$, **$P < 0.01$, ***$P < 0.001$.

injury. Recent studies also suggested that HIF-1α activation inhibited ferroptotic cell death of cardiomyocytes and neurons.[31,32] Furthermore, we observed significant alterations in the expression of GPX4 and ACSL4 after regulating HIF-1α, suggesting that the ferroptosis pathway GPX4/ACSL4 was the downstream target of HIF-1α in our model.
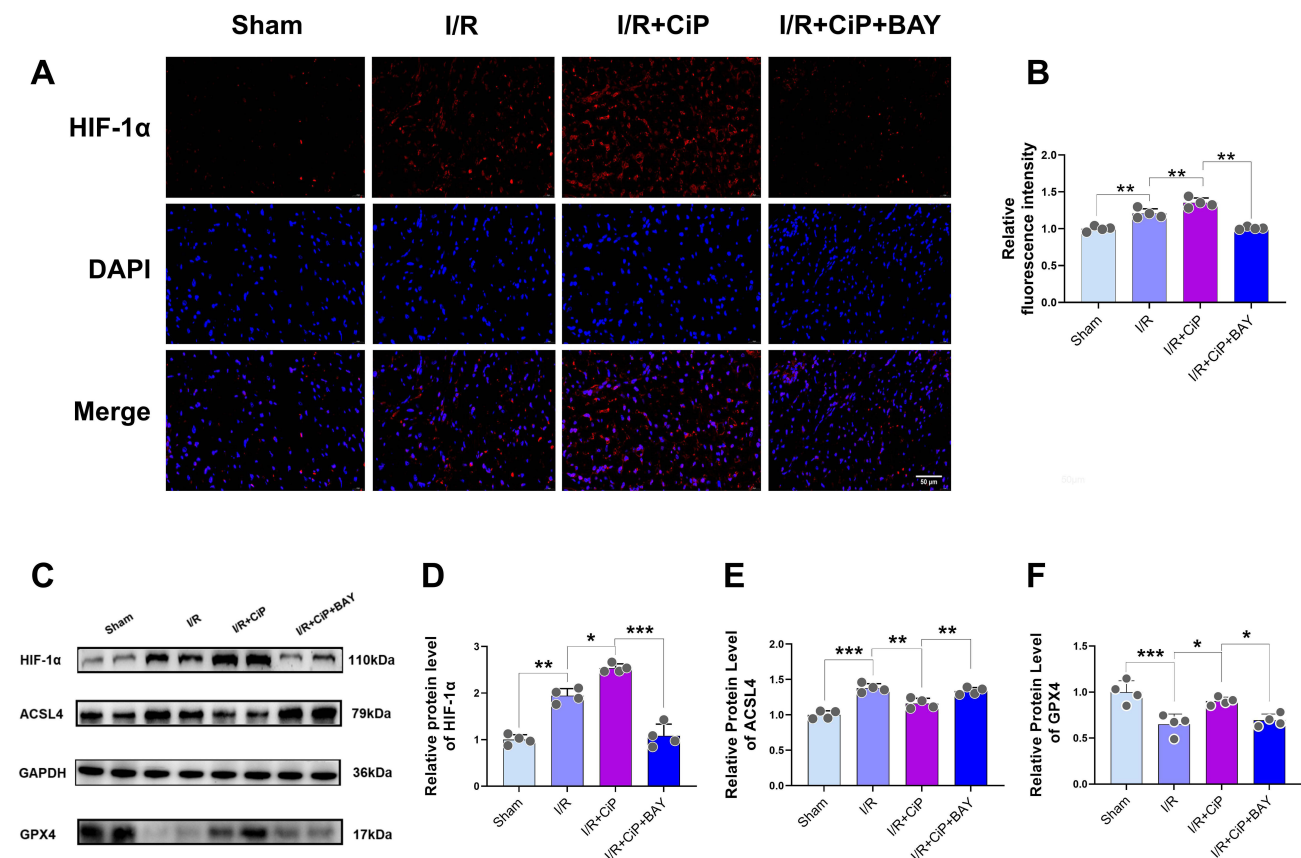
Figure 12 Ciprofol inhibited I/R-induced myocardial ferroptosis in mice by upregulating HIF-1α. BAY87-2243 (9 mg/kg i.g.) was administered daily for 3 days prior to ischemia. (**A** and **B**) Representative images and fluorescence intensity of HIF-1α expression in myocardium. Scale bar = 50 μm. (**C**–**F**) Western blot bands and quantification of HIF-1α, ACSL4, and GPX4 protein expression. Data are shown as mean ± SD (n = 4). *$P < 0.05$, **$P < 0.01$, ***$P < 0.001$.

Ciprofol is a newly developed intravenous anesthetic derived from propofol, exhibiting a 4–5 times greater anesthetic efficacy, reduced injection pain, and a good safety profile.[33,34] Dose adjustment was not required for the administration of ciprofol in patients with mild to moderate renal function impairment.[35] Regarding its effects on organ function, ciprofol has been shown to exert neuroprotection against cerebral I/R injury in mice;[36] another study suggested that ciprofol could mitigate myocardial damage but did not explore underlying mechanisms.[37] We found that ciprofol reduced CK-MB and cTnI levels and improved cardiac function in mice with myocardial I/R injury. Given the importance of cardiac and brain functions in anesthesia care, the potential advantages of using ciprofol in clinical settings are noteworthy.[38]

According to the literature, the conversion of drug doses from animals to humans should be calculated on the basis of the body surface area correction factor.[39,40] For a drug administered in mice, the human equivalent dose is calculated by dividing the mouse dose by 12.3. Thus, for ciprofol 10 mg/kg in mice, the human equivalent dose is 0.81 mg/kg. This ciprofol dose is clinically relevant. For patients undergoing surgery, ciprofol 0.4 mg/kg is normally used for anesthesia induction, followed by 0.8–2.4 mg/kg/h for anesthesia maintenance.[14,34] For the cell experiments, we explored the effects of different concentrations of ciprofol on cell viability of cultured cardiomyocytes in the normal condition and during H/R. Based on our observations, administering ciprofol (10 μM) exerted a significant protection against H/R-induced cell injury. Nonetheless, a high dose of ciprofol may have cell toxicity, as reflected by a reduction in cell viability after the use of ciprofol (50 and 100 μM) in cardiomyocytes.

Our findings provide the molecular basis for performing general anesthesia with ciprofol in surgical patients who are at increased risk of myocardial I/R injury, such as patients with ischemic heart disease or undergoing cardiac surgery with cardiopulmonary bypass. Administration of ciprofol during anesthesia induction and maintenance for those patients may help to prevent or alleviate subsequent myocardial injury during surgery and postoperatively. However, using anesthetics
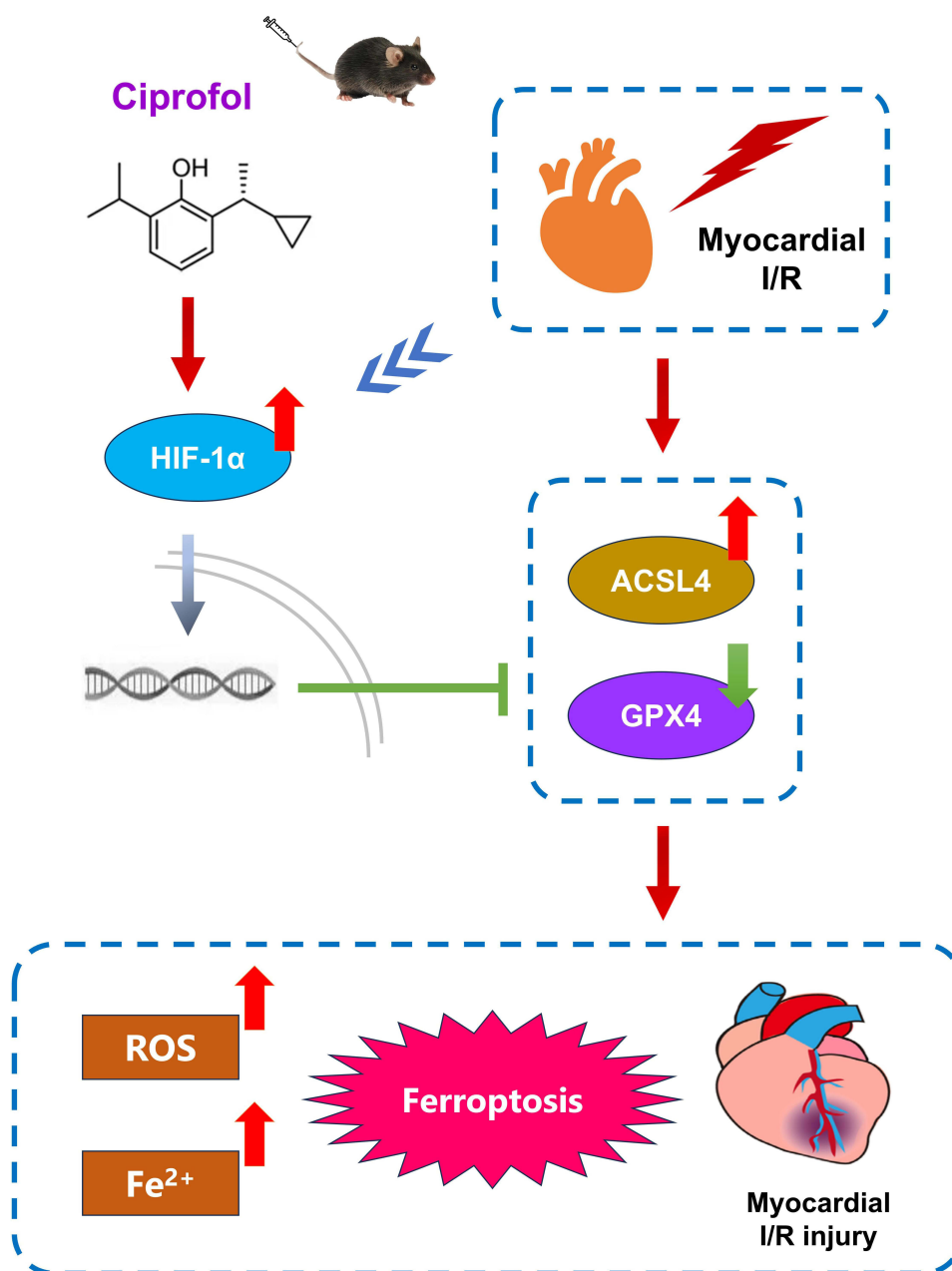
Figure 13 Schematic mechanism for the cardioprotection of ciprofol against I/R-induced myocardial ferroptosis in mice through upregulating HIF-1α.

to treat cardiovascular diseases such as myocardial infarction is not our primary intention, and thus the feasibility of application of anesthetic agents in such clinical scenarios needs to be tested by more clinical studies.

Our study has several limitations. First, we used H9c2 cells instead of primary neonatal mouse cardiomyocytes; however, we also performed in vivo study in mice. Second, our results demonstrated that ciprofol inhibited ferroptosis to protect the heart via activating HIF-1α and regulating the expression of GPX4 and ACSL4. We showed that the classical GPX4/ACSL4 ferroptosis pathway was the downstream of HIF-1α, but how ciprofol affected the expression of HIF-1α requires further research. Third, we mainly focused on the critical role of ferroptosis in the pathological process of myocardial I/R injury in our models, whereas other types of cell death (such as apoptosis and necrosis) may also be involved. A recent study suggested that ciprofol attenuated isoproterenol-induced oxidative damage, inflammation, and apoptosis of cardiomyocytes.[37] Next, several groups had a small size (n = 4) due to limited sample availability. To allow for meaningful statistical analysis, we have utilized the permutation test to compared these groups. Last, whether the

protection offered by ciprofol would be greater than that by propofol against myocardial I/R injury warrants future studies.

In conclusion, this experimental study demonstrated that ciprofol protected the mouse heart against I/R injury by inhibition of ferroptosis through upregulating HIF-1α expression (Figure 13). Our findings offer a new perspective on the clinical use of ciprofol for perioperative cardiac protection.

Data Sharing Statement

Data will be available on reasonable request from Dr. Peng (pengke0422@163.com).

Acknowledgments

Disclosure

The authors declare that they have no competing interests within this work.

References

1. Diseases GBD, Injuries C. Global burden of 369 diseases and injuries in 204 countries and territories, 1990-2019: a systematic analysis for the global burden of disease study 2019. *Lancet*. 2020;396(10258):1204–1222. doi:10.1016/S0140-6736(20)30925-9
2. Marijon E, Narayanan K, Smith K, et al. The lancet commission to reduce the global burden of sudden cardiac death: a call for multidisciplinary action. *Lancet*. 2023;402(10405):883–936. doi:10.1016/S0140-6736(23)00875-9
3. Alexander T, Kumbhani DJ, Mullasari Sankardas A. The future of pharmacoinvasive therapy for st-segment-elevation myocardial infarction reperfusion in the post-STREAM era. *Circulation*. 2024;149(10):732–733. doi:10.1161/CIRCULATIONAHA.123.066703
4. Del Re DP, Amgalan D, Linkermann A, Liu Q, Kitsis RN. Fundamental mechanisms of regulated cell death and implications for heart disease. *Physiol Rev*. 2019;99(4):1765–1817. doi:10.1152/physrev.00022.2018
5. Zhang Q, Wang L, Wang S, et al. Signaling pathways and targeted therapy for myocardial infarction. *Signal Transduct Target Ther*. 2022;7(1):78. doi:10.1038/s41392-022-00925-z
6. Liu S, Bi Y, Han T, et al. The E3 ubiquitin ligase MARCH2 protects against myocardial ischemia-reperfusion injury through inhibiting pyroptosis via negative regulation of PGAM5/MAVS/NLRP3 axis. *Cell Discov*. 2024;10(1):24. doi:10.1038/s41421-023-00622-3
7. Hernandez-Resendiz S, Prakash A, Loo SJ, et al. Targeting mitochondrial shape: at the heart of cardioprotection. *Basic Res Cardiol*. 2023;118 (1):49. doi:10.1007/s00395-023-01019-9
8. Qin L, Ren L, Wan S, et al. Design, synthesis, and evaluation of novel 2,6-disubstituted phenol derivatives as general anesthetics. *J Med Chem*. 2017;60(9):3606–3617. doi:10.1021/acs.jmedchem.7b00254
9. Zhong J, Zhang J, Fan Y, et al. Efficacy and safety of ciprofol for procedural sedation and anesthesia in non-operating room settings. *J Clin Anesth*. 2023;85:111047. doi:10.1016/j.jclinane.2022.111047
10. Wu B, Zhu W, Wang Q, Ren C, Wang L, Xie G. Efficacy and safety of ciprofol-remifentanil versus propofol-remifentanil during fiberoptic bronchoscopy: a prospective, randomized, double-blind, non-inferiority trial. *Front Pharmacol*. 2022;13:1091579. doi:10.3389/fphar.2022.1091579
11. Liu L, Wang K, Yang Y, et al. Population pharmacokinetic/pharmacodynamic modeling and exposure-response analysis of ciprofol in the induction and maintenance of general anesthesia in patients undergoing elective surgery: a prospective dose optimization study. *J Clin Anesth*. 2024;92:111317. doi:10.1016/j.jclinane.2023.111317
12. Liu Y, Peng Z, Liu S, et al. Efficacy and safety of ciprofol sedation in ICU patients undergoing mechanical ventilation: a multicenter, single-blind, randomized, noninferiority trial. *Crit Care Med*. 2023;51(10):1318–1327. doi:10.1097/CCM.0000000000005920
13. Sun X, Zhang M, Zhang H, Fei X, Bai G, Li C. Efficacy and safety of ciprofol for long-term sedation in patients receiving mechanical ventilation in ICUs: a prospective, single-center, double-blind, randomized controlled protocol. *Front Pharmacol*. 2023;14:1235709. doi:10.3389/fphar.2023.1235709
14. Liang P, Dai M, Wang X, et al. Efficacy and safety of ciprofol vs. propofol for the induction and maintenance of general anaesthesia: a multicentre, single-blind, randomised, parallel-group, Phase 3 clinical trial. *Eur J Anaesthesiol*. 2023;40(6):399–406. doi:10.1097/EJA.0000000000001799
15. Chen J, Li X, Zhao F, Hu Y. HOTAIR/miR-17-5p axis is involved in the propofol-mediated cardioprotection against ischemia/reperfusion injury. *Clin Interv Aging*. 2021;16:621–632. doi:10.2147/CIA.S286429
16. Lu Z, Liu Z, Fang B. Propofol protects cardiomyocytes from doxorubicin-induced toxic injury by activating the nuclear factor erythroid 2-related factor 2/glutathione peroxidase 4 signaling pathways. *Bioengineered*. 2022;13(4):9145–9155. doi:10.1080/21655979.2022.2036895
17. Wu X, Li Y, Zhang S, Zhou X. Ferroptosis as a novel therapeutic target for cardiovascular disease. *Theranostics*. 2021;11(7):3052–3059. doi:10.7150/thno.54113

18. Cai W, Liu L, Shi X, et al. Alox15/15-HpETE aggravates myocardial ischemia-reperfusion injury by promoting cardiomyocyte ferroptosis. *Circulation*. 2023;147(19):1444–1460. doi:10.1161/CIRCULATIONAHA.122.060257

19. Ju J, Li XM, Zhao XM, et al. Circular RNA FEACR inhibits ferroptosis and alleviates myocardial ischemia/reperfusion injury by interacting with NAMPT. *J Biomed Sci*. 2023;30(1):45. doi:10.1186/s12929-023-00927-1

20. Wang Y, Zhang M, Bi R, et al. ACSL4 deficiency confers protection against ferroptosis-mediated acute kidney injury. *Redox Biol*. 2022;51:102262. doi:10.1016/j.redox.2022.102262

21. Cao L, Liu J, Ye C, Hu Y, Qin R. Caffeic acid inhibits Staphylococcus aureus-induced endometritis through regulating AMPKalpha/mTOR/HIF-1alpha signalling pathway. *J Cell Mol Med*. 2024;28(20):e70175. doi:10.1111/jcmm.70175

22. Shi J, Song S, Wang Y, et al. Esketamine alleviates ferroptosis-mediated acute lung injury by modulating the HIF-1alpha/HO-1 pathway. *Int Immunopharmacol*. 2024;142(Pt A):113065. doi:10.1016/j.intimp.2024.113065

23. Yang X, Wu J, Cheng H, Chen S, Wang J. Dexmedetomidine ameliorates acute brain injury induced by myocardial ischemia-reperfusion via upregulating the Hif-1 pathway. *Shock*. 2023;60(5):678–687. doi:10.1097/SHK.0000000000002217

24. Miyamoto HD, Ikeda M, Ide T, et al. Iron overload via heme degradation in the endoplasmic reticulum triggers ferroptosis in myocardial ischemia-reperfusion injury. *JACC Basic Transl Sci*. 2022;7(8):800–819. doi:10.1016/j.jacbts.2022.03.012

25. Lei X, Teng W, Fan Y, et al. The protective effects of HIF-1alpha activation on sepsis induced intestinal mucosal barrier injury in rats model of sepsis. *PLoS One*. 2022;17(5):e0268445. doi:10.1371/journal.pone.0268445

26. Du J, Wang C, Chen Y, et al. Targeted downregulation of HIF-1alpha for restraining circulating tumor microemboli mediated metastasis. *J Control Release*. 2022;343:457–468. doi:10.1016/j.jconrel.2022.01.051

27. Qian W, Liu D, Han Y, et al. Cyclosporine A-loaded apoferritin alleviates myocardial ischemia-reperfusion injury by simultaneously blocking ferroptosis and apoptosis of cardiomyocytes. *Acta Biomater*. 2023;160:265–280. doi:10.1016/j.actbio.2023.02.025

28. Yan J, Li Z, Liang Y, et al. Fucoxanthin alleviated myocardial ischemia and reperfusion injury through inhibition of ferroptosis via the NRF2 signaling pathway. *Food Funct*. 2023;14(22):10052–10068. doi:10.1039/d3fo02633g

29. Li S, Lei Z, Yang X, et al. Propofol protects myocardium from ischemia/reperfusion injury by inhibiting ferroptosis through the AKT/p53 signaling pathway. *Front Pharmacol*. 2022;13:841410. doi:10.3389/fphar.2022.841410

30. Knutson AK, Williams AL, Boisvert WA, Shohet RV. HIF in the heart: development, metabolism, ischemia, and atherosclerosis. *J Clin Invest*. 2021;131(17). doi:10.1172/JCI137557

31. Ge C, Peng Y, Li J, et al. Hydroxysafflor yellow a alleviates acute myocardial ischemia/reperfusion injury in mice by inhibiting ferroptosis via the activation of the HIF-1alpha/SLC7A11/GPX4 signaling pathway. *Nutrients*. 2023;15(15):3411. doi:10.3390/nu15153411

32. An S, Shi J, Huang J, Li Z, Feng M, Cao G. HIF-1alpha induced by hypoxia promotes peripheral nerve injury recovery through regulating ferroptosis in DRG neuron. *Mol Neurobiol*. 2024;61(9):6300–6311. doi:10.1007/s12035-024-03964-5

33. Chen L, Xie Y, Du X, et al. The effect of different doses of ciprofol in patients with painless gastrointestinal endoscopy. *Drug Des Devel Ther*. 2023;17:1733–1740. doi:10.2147/DDDT.S414166

34. Ding YY, Long YQ, Yang HT, Zhuang K, Ji FH, Peng K. Efficacy and safety of ciprofol for general anaesthesia induction in elderly patients undergoing major noncardiac surgery: a randomised controlled pilot trial. *Eur J Anaesthesiol*. 2022;39(12):960–963. doi:10.1097/EJA.0000000000001759

35. Qin K, Qin WY, Ming SP, Ma XF, Du XK. Effect of ciprofol on induction and maintenance of general anesthesia in patients undergoing kidney transplantation. *Eur Rev Med Pharmacol Sci*. 2022;26(14):5063–5071. doi:10.26355/eurrev_202207_29292

36. Liu X, Ren M, Zhang A, Huang C, Wang J. Nrf2 attenuates oxidative stress to mediate the protective effect of ciprofol against cerebral ischemia-reperfusion injury. *Funct Integr Genomics*. 2023;23(4):345. doi:10.1007/s10142-023-01273-z

37. Yang Y, Xia Z, Xu C, Zhai C, Yu X, Li S. Ciprofol attenuates the isoproterenol-induced oxidative damage, inflammatory response and cardiomyocyte apoptosis. *Front Pharmacol*. 2022;13:1037151. doi:10.3389/fphar.2022.1037151

38. Liu Z, Jin Y, Wang L, Huang Z. The effect of ciprofol on postoperative delirium in elderly patients undergoing thoracoscopic surgery for lung cancer: a prospective, randomized, controlled Trial. *Drug Des Devel Ther*. 2024;18:325–339. doi:10.2147/DDDT.S441950

39. Nair AB, Jacob S. A simple practice guide for dose conversion between animals and human. *J Basic Clin Pharm*. 2016;7(2):27–31. doi:10.4103/0976-0105.177703

40. Reagan-Shaw S, Nihal M, Ahmad N. Dose translation from animal to human studies revisited. *FASEB J*. 2008;22(3):659–661. doi:10.1096/fj.07-9574LSF